试样尺寸对 SA508-3 钢焊接接头断裂韧度的影响

杜 兵[1,2]， 孙凤莲[1]， 李小宇[2]， 孙静涛[2]， 吕晓春[2]
(1. 哈尔滨理工大学，哈尔滨 150001; 2. 哈尔滨焊接研究所，哈尔滨 150028)

摘 要: 针对大型核容器 SA508-3 钢焊接接头断裂韧度进行了研究. 结果表明，在大试样条件下，母材、焊缝金属及热影响区的断裂韧度存在差异，焊缝金属的断裂韧度优于热影响区，母材的断裂韧度最低. 试样几何尺寸直接影响裂纹尖端的应力状态，小试样时裂纹尖端处于平面应力状态，母材、焊缝金属及热影响区全部呈韧窝断裂，表现出良好的塑性; 大试样时裂纹尖端处于平面应变状态，母材断口特征转变为准解理与解理混合断裂，热影响区为典型的准解理断裂，焊缝为韧窝断裂.

关键词: SA508-3 钢; 断裂韧度; 焊接接头; 试样尺寸
中图分类号: TG 404 **文献标识码**: A **文章编号**: 0253 - 360X(2014)06 - 0001 - 04

0 序 言

中国是能源消费大国，为保障国家能源安全，坚持绿色可持续发展，近年来持续兴建大型核电站. 然而，由于日本福岛核电事故造成严重的核泄漏污染，世界各国更加重视核电的安全发展，对核级设备的制造质量提出了更高要求.

SA508-3 钢是国际上主流的核电压力容器用钢[1-3]. 国内也成功研制出大型核电压力容器用 SA508-3 锻钢并用于 1000 MW 压力壳等核岛设备的制造. 核电压力容器作为整个核电设备的心脏，由于尺寸大、结构复杂，通常采用锻焊结构. 从设计与选材角度，断裂韧度分析已成为核电压力容器选材和设计的基础，在美国标准 ASME 规范中有明确的要求. 对于断裂韧度的试验分析，由于 SA508-3 钢的设计强度并不很高，塑性与韧性非常好，因此，若按照弹性断裂力学理论估算试样尺寸，将需要较大尺寸，这不仅造成试验费用巨大，相应的试验设备也缺乏. 目前常用的方法是利用小试样(试样厚度一般不超过 30 mm)获得试验数据，然后进行计算分析，进而对安全可靠性做出判断. 有研究指出，试样尺寸对断裂韧度的特征值影响不大，但对断裂机制还不清楚[4,5]. 同时，研究大多集中于母材，有关焊接接头的断裂韧度研究也相对缺乏[6]. 因此，文中一方面开展焊接接头断裂韧度研究，对比分析母材、热影响区及焊缝金属断裂韧度的差异，另一方面分析试样尺寸对 SA508-3 钢焊接接头断裂韧度的影响.

收稿日期: 2014 - 03 - 01
基金项目: 国家科技重大专项资助项目(2011ZX04016 - 061)

1 试验方法

试验母材为国产核电压力容器用 SA508-3 钢，化学成分与力学性能分别见表 1 和表 2. 试板尺寸为 800 mm × 600 mm × 100 mm. 采用窄间隙埋弧自动焊的方法进行平板对接焊，焊接材料采用 US-620 (ϕ4.0 mm) + PF-200(烧结焊剂). 焊接工艺参数见表 3. 焊后热处理工艺为 615 ℃ × 29 h，熔敷金属的化学成分与力学性能分别见表 4 和表 5.

表 1 SA508-3 钢的化学成分(质量分数，%)
Table 1 Chemical compositions of SA508-3 steel

C	Si	Mn	S	P	Cr	Ni	Mo	Fe
0.21	0.36	1.38	0.003 8	0.019	0.22	0.60	0.49	余量

表 2 SA508-3 钢的力学性能
Table 2 Mechanical properties of SA508-3 steel

抗拉强度 R_m/MPa	屈服强度 R_{eL}/MPa	断后伸长率 A(%)	断面收缩率 Z(%)	冲击吸收功 $A_{KV(0℃)}$/J
750	620	19.5	71.0	118

焊后按图 1 制取三点弯曲试样进行断裂韧性测试，试验温度为 0 ℃. 断裂韧度测试包括 SA508-3 钢母材、焊缝中心及焊接热影响区(距离表观熔合线 0.5 mm). 基于实测的母材屈服强度远高于技术指标要求，文中试验进行了平面应变断裂韧度 K_{IC} 的测

表 3 窄间隙埋弧自动焊焊接工艺参数

Table 3 Welding parameters of narrow-gap submerged arc welding

焊道	焊接电流 I/A	电弧电压 U/V	焊接速度 v/(mm·min^{-1})	预热温度 T/℃
根部封底	480	28 ~ 30	350	200 ~ 250
后续各道	500	28 ~ 30	350	175 ~ 230

表 4 US-620/PF-200 熔敷金属化学成分(质量分数,%)

Table 4 Chemical compositions of US-620/PF-200 deposited metal

C	Si	Mn	S	P	Cr	Ni	Mo
0.11	0.17	1.12	0.008	0.013	0.02	0.48	0.29

表 5 熔敷金属力学性能

Table 5 Mechanical properties of deposited metal

抗拉强度 R_m/MPa	屈服强度 R_{eL}/MPa	断后伸长率 A(%)	断面收缩率 Z(%)	冲击吸收功 $A_{KV(0℃)}$/J
565	470	25.5	70	198

试. 对于焊缝与热影响区,考虑到实测的熔敷金属屈服强度较低及热影响区组织性能复杂,采用了多试样裂纹张开位移阻力曲线测试. 断裂试验后采用 SEM 进行断口分析,图 1 中 $W = 120$ mm 为试样宽度,$B = 30$ mm 和 60 mm 为试样厚度,$L_1 = 520$ mm 为试样长度,$L_2 = 12$ mm 为燕尾槽顶端宽度,$\alpha = 45°$ 为试样燕尾角度数,$a = 58$ mm 为试样裂纹长度.

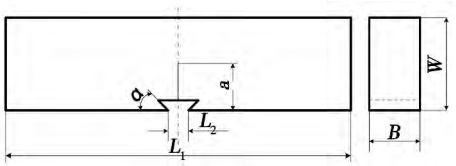

图 1 断裂韧度试样

Fig. 1 Three-point bending specimen for fracture toughness

2 试验结果与分析

表 6 为母材断裂韧度的试验结果,从母材的试验结果来看,根据国家标准 GB/T21143—2007《金属材料准静态断裂韧度的统一试验方法》判定,试验获得的平面应变断裂韧度的条件值 K_q,K_q 平均值符合 K_{IC} 有效性的两个条件. 由试验结果可见,K_{IC} 并不高,而且相对分散,反映出断裂过程的不稳定.

从试样 SEM 断口可以看出(图 2),由于试样尺寸的变化,使得裂纹尖端的受力状态由平面应力状态转变为平面应变状态,应力状态不同导致断裂机制也发生显著变化. 当采用较小试样($B = 30$ mm)时,裂纹尖端处于平面应力状态时,表现为韧窝断裂(图 2a);当采用较大试样时,裂纹尖端处于平面应变状态时,表现为准解理与解理的混合断裂模式.

表 6 母材断裂韧度试验结果

Table 6 Experimental results of fracture toughness for base metal

试样编号	应力强度 K_Q/(N·mm$^{-3/2}$)	应力强度平均值 $\overline{K}_Q$/(N·mm$^{-3/2}$)
1	73.9	
2	121.0	
3	119.0	88.38
4	61.8	
5	66.2	

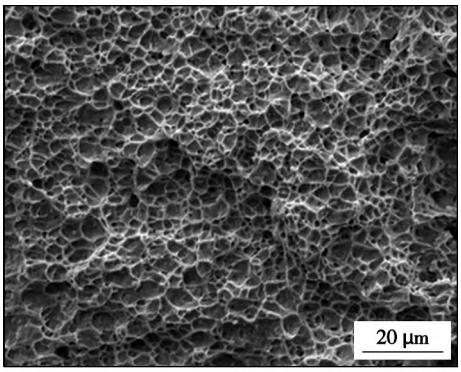

(a) 试样厚度 B=30 mm

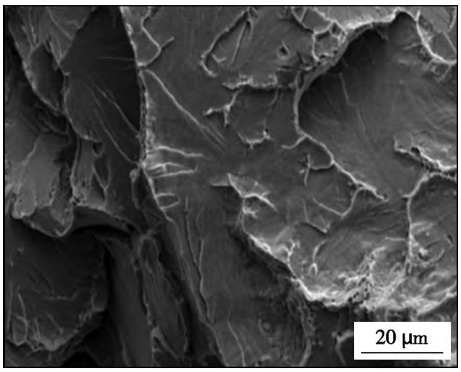

(b) 试样厚度 B=60 mm

图 2 母材断裂韧度试样断口分析

Fig. 2 SEM photograph of fracture toughness specimen for base metal

对于焊缝金属与热影响区,由于屈服强度较低,即使采用 60 mm 厚的试样也难以满足 K_{IC} 有效性的条件,所以直接检测裂纹扩展位移,表 7 为焊缝和热影响区裂纹尖端张开位移裂纹尖端张开位移 CTOD 的试验结果.

从焊缝金属试验结果看,断裂韧度比较高,启裂区为准解理与韧窝的混合断裂; 裂纹扩展区为韧窝

表 7　焊缝和热影响区的 CTOD 试验结果

Table 7　Experimental results of CTOD for weld metal and HAZ

缺口位置	条件启裂裂纹尖端张开位移值 $\delta_{0.2}$/mm	最大载荷裂纹尖端张开位移值 δ_m/mm
焊缝	0.97	1.84
热影响区	0.62	1.58

断裂,表现出较好的塑韧性(图 3). 从焊接热影响区试验结果看,断裂韧度比焊缝金属低,启裂区为韧窝断裂,同时发现一些球形的夹杂物和低熔点物质形成的空穴; 裂纹扩展区为典型的准解理断裂,如图4所示. 当采用小试样($B = 30$ mm)时,无论焊缝金属,还是热影响区均为韧窝断裂.

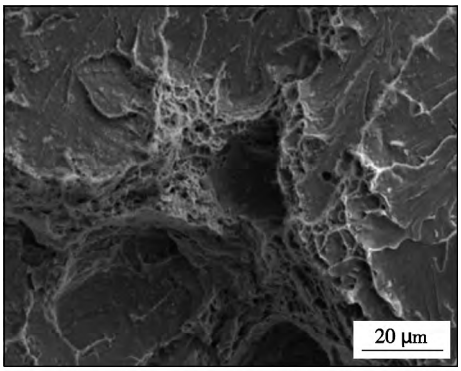

(a) B=60 mm时微观启裂区

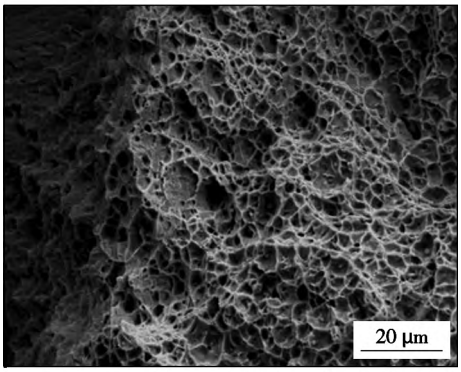

(b) B=60 mm时裂纹扩展区

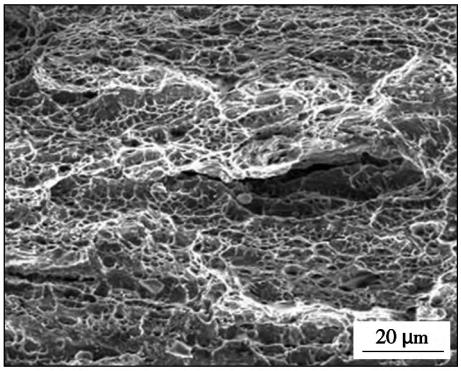

(c) B=30 mm时裂纹扩展区

图 3　焊缝金属断裂韧度试样表面断口分析

Fig. 3　SEM photograph of fracture toughness specimen for weld metal

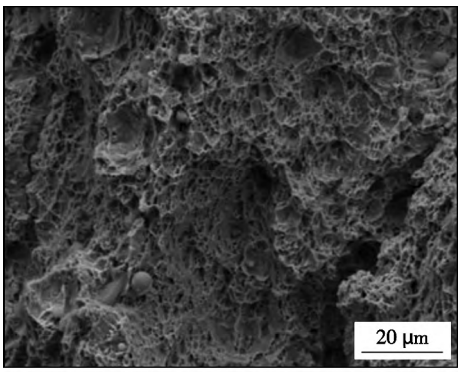

(a) B=60 mm时启裂区

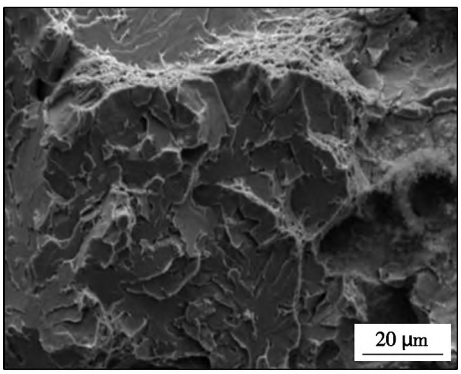

(b) B=60 mm时裂纹扩展区

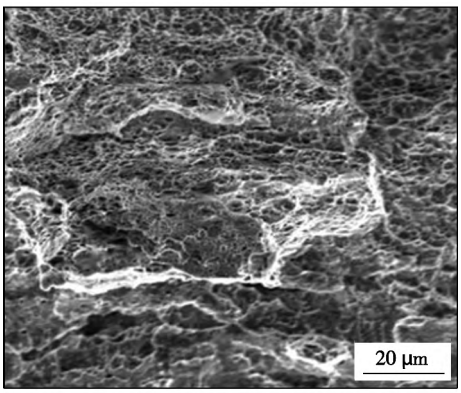

(c) B=30 mm时裂纹扩展区

图 4　热影响区断裂韧度试样表面断口分析

Fig. 4　SEM photograph of fracture toughness specimen for HAZ

结合断裂韧度特征值和断口特征综合分析,试验获得的断裂韧度值、断口特征与裂纹尖端应力状态具有很好的一致性. 焊缝金属的断裂韧度优于热影响区,母材的断裂韧度最低. 由此可见,母材的冶金质量还需进一步提升,包括杂质偏析的控制,晶粒的细化等. 以往采用小试样时,焊缝金属、热影响区及母材在断裂韧度方面的差异并不突出,在试验中采用较大试样时,三者的差别是比较明显的. 因此,在分析核电压力容器的安全可靠性时,应充分考虑小试样数据带来的盲目乐观.

3 结 论

(1) 在大试样条件下,母材、焊缝金属及热影响区的断裂韧度存在差异,焊缝金属的断裂韧度优于热影响区,母材的断裂韧度最低.

(2) 试样几何尺寸直接影响裂纹尖端的应力状态,小试样时裂纹尖端处于平面应力状态,母材、焊缝金属及热影响区全部呈韧窝断裂,表现出良好的塑性;大试样时裂纹尖端处于平面应变状态,母材断口特征转变为准解理与解理混合断裂,热影响区为典型的准解理断裂,焊缝为韧窝断裂.

参考文献:

[1] 迟露鑫,麻永林,刑淑清,等. 核电SA508-3钢焊接连续冷却转变曲线的分析[J]. 焊接学报,2011,32(5):61-64.
Chi Luxin, Ma Yonglin, Xing Shuqing, *et al*. Analysis on continues cooling transformation curves of sinulated heat affected zone for SA508-3 steel in nuclear power [J]. Transactions of the China Welding Institution, 2011, 32(5): 61-64.

[2] 张显辉,焦 伟,谭长瑛. 20MnNiMo钢焊接热影响区的组织和韧性及其氢致裂纹特征[J]. 焊接学报,2000,21(1):9-12.
Zhang Xianhun, Jiao Wei, Tan Changyin. HAZ structure, toughness and characteristics to hydrogen-induced cracking (HIC) of steel 20MnNiMo [J]. Transactions of the China Welding Institution, 2000, 21(1): 9-12.

[3] 迟露鑫,麻永林,刑淑清,等. 核电SA508-3钢厚壁圆筒纵向焊接残余应力分析[J]. 焊接学报,2012,33(6):59-67.
Chi Luxin, Ma Yonglin, Xing Shuqing, *et al*. Numerical simulation and experiments test of residual stress of longitudinal weld of thick SA508-3 steel pipe for nuclear power [J]. Transactions of the China Welding Institution, 2012,33(6): 59-67.

[4] 包章根,陆 斌,史巨元. 国产508-Ⅲ钢低周疲劳和动态断裂韧度试验研究[J]. 核动力工程,1999,20:244-247.
Bao Zhanggen, Lu Bin, Shi Juyuan. Test research for low cycle fatigue and dynamics fracture toughness of native 508-Ⅲ steel [J]. Nuclear Power Engineering, 1999, 20: 244-247.

[5] 郑隆滨,陈家伦,龚正春,等. 核电设备用SA508-3钢的研究[J]. 锅炉制造,1999,3:43-49.
Zheng Longbin, Chen Jialun, Gong Zhengchun, *et al*. Reserch of SA508-3 steel for nuclear power plant equipment [J]. Nuclear Power Engineering, 1999, 3: 43-49.

[6] Sangho Kim, Sukyoung Kang, Sunghak Lee, *et al*. Correlation of the microstructure and fracture toughness of the heat-affected zones of SA 508 steel [J]. Metallurgical and Materials Transactions, 2000, 3: 17-19.

作者简介: 杜 兵,男,1962年出生,研究员. 主要从事不锈钢、低合金钢、镍基合金、异种钢等焊接冶金、焊接材料和焊接新技术、钎焊材料及钎焊标准化等领域的研究. 获得国家科技进步奖2项,省部级科技进步奖6项,其它科技进步奖12项. 撰写专著2部,发表论文30余篇. Email: edwarddb@163.com

MAIN TOPICS, ABSTRACTS & KEY WORDS

Effect of sample size on fracture toughness of SA508-3 steel welded joint DU Bing[1,2], SUN Fenglian[1], LI Xiaoyu[2], SUN Jingtao[2], LÜ Xiaochun[2] (1. Harbin University of Science and Technology, Harbin 150001, China; 2. Harbin Welding Institute, Harbin 150028, China). pp 1 - 4

Abstract: Fracture toughness of SA508-3 steel welded joints was investigated for large nuclear vessel. The results show that the fracture toughness was different for base metal, weld metal and heat affected zone with larger sample size. The weld metal had superior fracture toughness compared to heat affected zone, and the fracture toughness of base metal was lowest. Sample size directly affected the stress state at the crack tip which endured plane stress in small sample. The base metal, weld metal and heat affected zone had good toughness with dimple fracture morphology. However, the crack tip in large sample endured plane strain condition. The fracture morphology of base metal presented quasi-cleavage and cleavage mixed mode. The heat affected zone was typical quasi-cleavage mode, and the weld metal revealed dimple fracture.

Key words: SA508-3 steel; fracture toughness; welded joint; sample size

Influence of preset gap on strength and failure mode of steel/aluminum CMT joint YANG Shuo, LIN Jian, LEI Yongping, KONG Dening (School of Material Science and Engineering, Beijing University of Technology, Beijing 100124, China). pp 5 - 8

Abstract: The strength and failure mode of dissimilar materials joint between galvanized low carbon steel and aluminum alloy made by cold metal transfer (CMT) welding process were investigated. In order to enlarge the bonded area of brazed joint, preset gap was introduced between steel and aluminum alloy during CMT welding processing by means of feeler. It is found that the shear strength of steel/aluminum CMT welded joint could be improved with increasing of preset gap because the length of bonded line was improved. When the preset gap was increased to 0.5 mm, brittle fracture occurred at the interface layer between steel and aluminum due to the existence of remained zinc at the weld toe.

Key words: cold metal transfer; preset gap; length of bonded line; failure mode

Reverse-driving trajectory planning of welding robot with NURBS SHAO Yuanyuan[1], XUAN Guantao[1], LIU Jing[2], HOU Jialin[1] (1. College of Mechanical and Electrical Engineering, Shandong Agricultural University, Tai'an 271018, China; 2. Department of Mechanical and Electrical Engineering, Shandong University of Science and Technology, Tai'an 271018, China). pp 9 - 12

Abstract: During solving inverse kinematics problems of welding robot, there are often multiple solutions or even no solution. A reverse-driving trajectory planning method based on ADAMS and MATLAB was put forward to overcome the above disadvantages. With the non-uniform rational B-splines (Non-Uniform Rational B-Splines, NURBS) as curve fitting tool, the kinematics simulation of welding robot was carried out. The results show that, compared to the sinusoidal curve and five-degree polynomial and other traditional planning algorithm, the joint angular displacement curve achieved by reverse-driving trajectory planning algorithm with NURBS was much better, the displacement error of manipulator in each direction was as small as less than 1 mm. Therefore, the desired trajectory of welding robot could be achieved quickly and accurately. This paper provided a new method for trajectory planning of welding robot.

Key words: reverse-driving; trajectory planning; non-uniform rational B-splines

Microstructure of friction welded joint between single crystal superalloy DD3 and fine grain superalloy FGH4095 DU Suigeng[1], WANG Xifeng[1], WANG Jinwei[2], JIANG Zhe[1] (1. Key Laboratory of Ministry of Education for Contemporary Design and Integrated Manufacturing Technology, Northwestern Polytechnical University, Xi'an 710072, China; 2. Chinese North Engine Research Institute, Datong 037036, China). pp 13 - 16

Abstract: The microstructure and composition of weld zone in friction welded joint between single crystal superalloy DD3 and powder fine grain superalloy FGH4095 were analyzed by metallographic microscope and SEM-EDS. The results indicate that the dynamic recrystallization grains form on both sides of the bonding interface, which had distinct boundary. In bonding zone, the alloying elements in single crystal superalloy and fine grain superalloy diffused to each other. The dynamic recrystallization grains of the dissimilar materials grew to each other by bow shape, and the tendency of FGH4095 dynamic recrystallization grain growing up to DD3 alloy was more than the opposite tendency. Through mutual grains, these two dissimilar materials were bonded. During friction welding, the friction interface transformed from the interface of DD3 and FGH4095 to the interior of DD3 friction band. The change of microstructure gradient in the joint was great.

Key words: blisk; friction welding; superalloy; single crystal superalloy; powder superalloy

Factors affecting welded joints geometry in temper bead welding technology QIN Jian[1], LÜ Xiaochun[1], DU Bing[1], HU Zhongquan[2] (1. Harbin Welding Institute, Harbin 150028,